Communication in Physical Science 2020, 5(3): 270-280 https://journalcps.com

Utilization of *Musanga cecropioides* wood saw dust for the removal of disperse yellow (DY) dye from aqueous solution

Anduang Ofuo Odiongenyi

Received 12 April 2020/Accepted 27 May 2020/Published online: 30 May 2020

Abstract In continuation of the research on sourcing for affordable, biodegradable and efficient adsorbents for dye in contaminated water, the present study was designed to investigate the adsorption efficiency of *Musanga cecropioides* wood saw dust for disperse yellow dye. Effects of adsorbent dosage, temperature, concentration of dye and period of contact were investigated using batch adsorption process. The results obtained indicated that the equilibrium amount of dye adsorbed were within the following ranges, 3.5313 to 39.1875, 9.03 to 23.06, 16.66 to 19.22 and from 16.72 to 18.47 mg/g with respect to concentration, adsorption dosage, period of contact and temperature respectively. The amount of dye adsorbed increases with adsorbent dosage but decreased with increase in temperature. The adsorption of the dye on the surface of the wood saw dust was spontaneous and obseyed the adsorption models of Langmuir, Freundlich, Javanovic, Redich-Peterson and Brouers-Sotolongo. FTIR study indicated that the major functional groups responsible for the adsorption of the dye were C-O and C=O functional groups, while other functional groups indicated the presence of interactions due to shift in frequencies. The study reveals that resource recovery practice from *Musanga cecropioides* wood saw dust can create an eco-friendly adsorbent for the purification of dye contaminated water.

Key Words: *Water contamination, dye,*

Anduang Ofuo Odiongenyi
Department of Chemistry
Akwa Ibom State University
Ikot Akpaden, Akwa Ibom State, Nigeria
Email: anduangodiong@gmail.com
Orcid id: 0000-0002-6842-9976

1.0 Introduction

Adsorption is a major phenomenon that has solved several environmental problems and it has been widely applied in decontamination of dye contaminated water (Eddy, 2009). The process involves the sticking of the adsorbate molecules (dye molecules) unto the surface of the adsorbent either through the mechanism of charge transfer (physisorption) or electron transfer (chemisorption) (Eddy *et al*., 2011). Dye contamination is a serious environmental nuisance because it can harshly influence the health of the aquatic environment through interference with light penetration, photosynthesis, colouration, reactions with other systems in the environment, etc. (Gopura *et al*., 2016).

In view of their tremendous success in reducing the negative impact of dye especially in aquatic environment, several adsorbents have been selected and implemented including human hair (Ekop and Eddy, 2020), plant waste (Munagapati *et al*., 2018), synthetic materials (Iqbal *et al*., 2011), nano materials (Odiongenyi, 2019; Odiongenyi and Afangide, 2019). Revathi *et* al. (2011) found that jack fruit leaf carbon is an efficient adsorbent for the removal of DY dye from aqueous solution. They observed that adsorption of the dye fitted some adsorption models including Langmuir, Freundlich and pseudo first order kinetic models. Palapa *et al*. (2018) reported that Ni/Al and Zn/Al layer double hydroxides are effective as adsorbents for the [illegible] solution. El Boujaady *et al*. (2014) reported good adsorption potential of apatitic tricalcium phosphate for the removal of direct yellow 28 (DY28) from aqueous solution and observed that the removal potential depends on pH, concentration and other variables. The adsorption fitted some adsorption and kinetic models and was spontaneous. FTIR study was informative in identifying the functional groups that were associated with the adsorption process. The present study was designed to facilitate and progress

the needs for resource recovery and utilization of cheap and ecofriendly adsorbent for the removal of disperse yellow dye from aqueous solution via adsorption.

2.0 Materials and Methods

The chemical structure of the dye used for the study is shown below

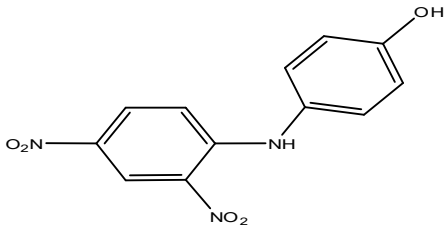

Chemical structure of DY dye (4-(2,4-dinitrophenylamino)phenol)

The dye sample and all other reagents were supplied by the Chemistry departmental store, Akwa Ibom State University. Saw dust were produced from *Musanga cecropiodes* wood. Experimental component of the work included batch adsorption experiment, spectrophotometric determination of concentration, FTIR analysis of functional groups and computational chemistry calculations.

2.1 Batch adsorption experiment

Batch adsorption process as reported elsewhere was used to study the effect of concentration, contact time, adsorbent dosage and temperature (Odoemelam *et al*. 2018). Equilibrium concentration of the dye was calculated using equation 1

$$q_e = \frac{C_0 - C_e}{C_0} \times \frac{V}{m} \qquad (1)$$

where C_0 is the initial concentration of the dye , C_e is the equilibrium concentration of the dye, V is the volume of solution and m is the mass of the adsorbent.

2.2 Spectrophotometric determination of dye concentration

All spectrophotometric analyses were carried out using 721,P/N:A003 UV-visible spectrophotometer In spectrophotometric analysis, wave length of maximum absorption of DY dye was measured. All measurements were carried out using the maximum wavelength of absorption of DY dye as the reference wave length (according to Beer-Lambert's law of spectrophotometry). Calibration curve was plotted and the concentration of the dye was obtained through extrapolation from the calibration curve shown in Fig. 1.

2.3 FTIR analysis

FTIR analysis of the dye, adsorbent (before and after adsorption) was carried out using Agilent FTIR spectrophotometer (Located in Chemistry Department of the Bayero University, Kano, Nigeria). The samples were prepared with KBr powder and the scan range was 650 to 4 000 cm^{-1}. The system status was good while the Apolization was Happ-Genzel. The Agilent Technologies software also provided provision for display of analytical output.

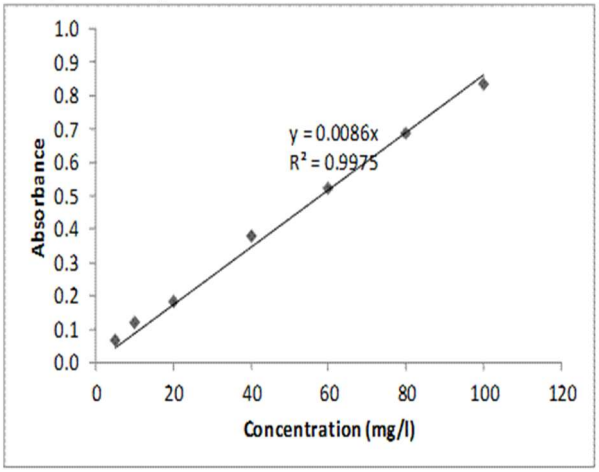

Fig. 1: Calibration curve for disperse yellow dye (DY dye)

3.0 Results and Discussion

3.1 Effect of concentration

Fig. 2 shows plots for the variation of equilibrium concentration of DY dye adsorbed (and also percentage of dye adsorbed) by the wood saw dust with concentration.

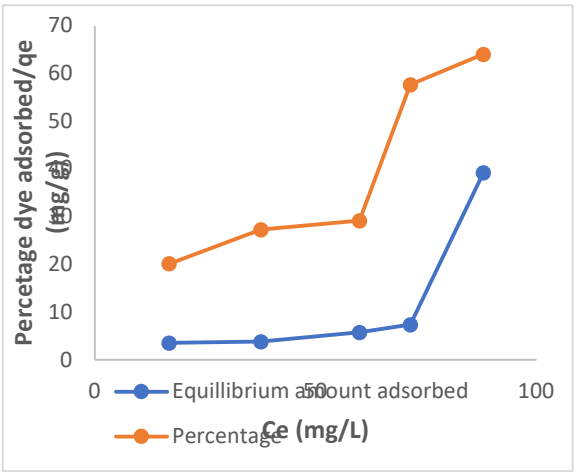

Fig. 2: Variation of amount of DY dye adsorbed with initial dye concentration

The plots reveal a rise in adsorption with increase in concentration. The wood saw dust has maximum adsorption site. Adsorption will prefer to increase as the amount of dye approaching the adsorbent surface by mass transport increases until adsorption equilibrium is established. Once equilibrium is achieved, further increase in adsorption will not lead to increase in the amount of dye adsorbed (Odoemelam *et al*., 2018).

3.2 Effect of period of contact

Adsorption is a function of time and has widely been established for various adsorption phenomena (Eddy *et al*., 2011; Odoemelam and Eddy, 2009). In this study, adsorption of DY dye onto wood saw dust rose with a pronounce increase in time and then progresses slowly with time (Fig. 3). The observed trend indicates that at first the vacant sites were competing for adsorbent but once the occupancy of the vacant sites started, then the slowing down of the rate at which the adsorption proceeds (Silva *et al*., 2019). Also, some adsorption sites can be interwoven, leading to reduction in adsorption with time (Dhaif-Allah *et al.,* 2020).

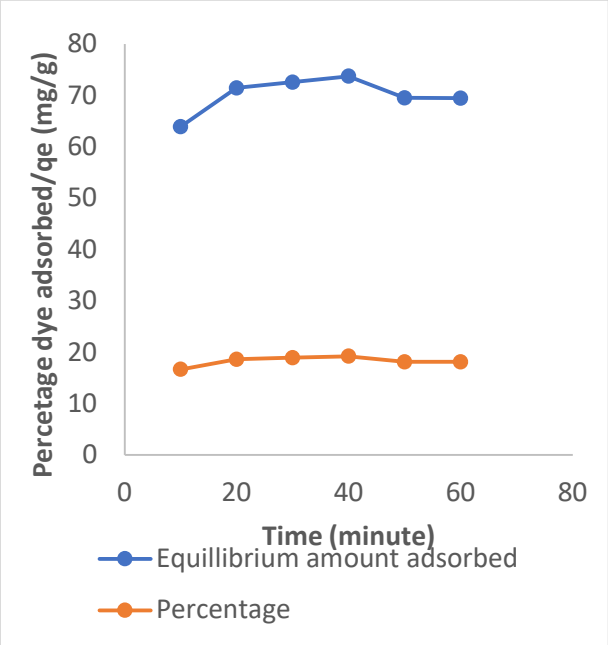

Fig. 3: Variation of amount of DY dye absorbed with time

3.3 Effect of temperature

In Fig. 4, it is evident that the amount of DY dye adsorbed on the surface of wood saw dust decreases with increase in temperature, which is evident of physisorption mechanism. According to Eddy *et al.* (2011), physical adsorption mechanism can be differentiated from chemical adsorption mechanism through the trend in variation of the extent of adsorption with temperature. An increase in extent of adsorption with temperature indicates chemical adsorption while a decrease in extent of adsorption with temperature is an indication of physical adsorption mechanism. Some studies on the adsorption of dyes has reported similar findings (Shoukat *et al.*, 2017; Weloye *et al*., 2020).

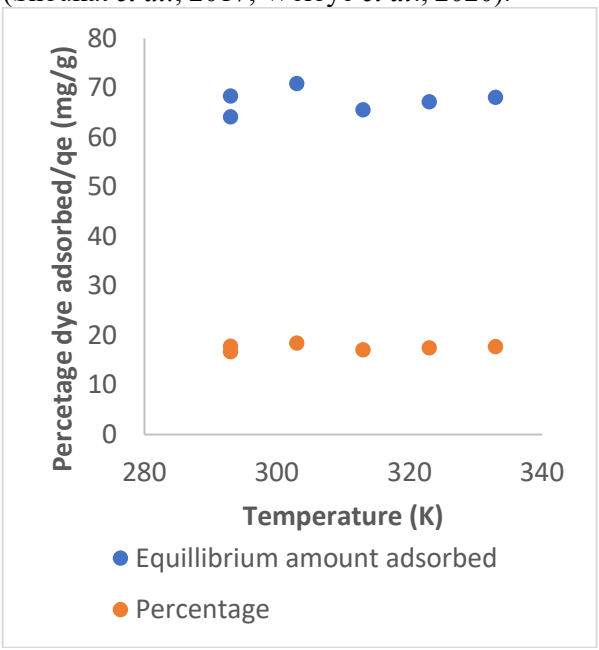

Fig. 4: Variation of amount of dye adsorbed with temperature

3.4 Effect of adsorbent dosage

Fig. 5 shows that the amount of dye adsorbed increases with increase in adsorbent dose

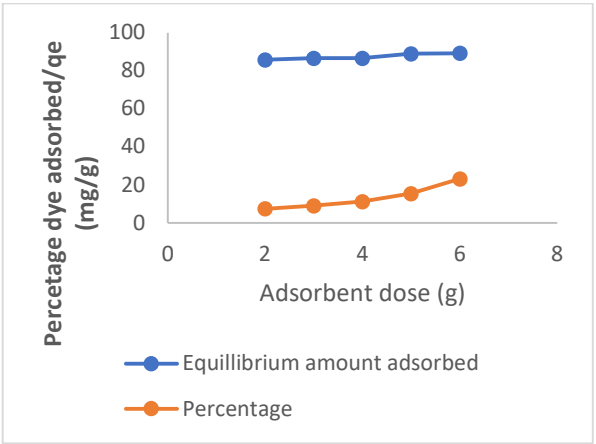

Fig. 5: Variation of amount of DY dye adsorbed with adsorbent dose

The increase can be attributed to increase in the number of adsorbent sites, which created increase degree of freedom for the adsorbate molecules to be trapped.

3.4 Adsorption isotherm

Adsorption isotherms can provide information on interaction between adsorbed species and on the adsorption behaviour of the dye. The adsorption data was fitted to different adsorption isotherms and the isotherms that gave highest values of degree of linearity (R^2) were retained.

The Langmuir adsorption isotherm assumes mono layer adsorption on the surface of the adsorbent having equivalent adsorption sites with uniform energies. The general form of the Langmuir isotherm is written according to equation 3 (Chiu *et al* ., 2018)'

$$q_e = \frac{Q_m k_{ads} C_e}{1 + k_{ads} C_e} \quad (2)$$

q_e is the equilibrium amount of dye adsorbed, k_{ads} is the Langmuir adsorption-desorption equilibrium constant, Q_m is the theoretical adsorption capacity and C_e is the equilibrium concentration. The essential feature of the Langmuir model is the separation factor (R_L), which is an index that defines favourable ($0<R_L<1$), linear ($R_L=1$), unfavourable ($R_L > 1$) or irreversible ($R_L =0$) (Odoemelam *et al., 2018*)

$$R_L = \frac{1}{1 + k_{ads} C_0} \quad (3)$$

Equation 3 can be simplified as follows,

$$\frac{q_e}{C_e} = \frac{Q_m k_{ads}}{1 + k_{ads} C_e} \quad (4)$$

$$\frac{C_e}{q_e} = \frac{1 + k_{ads} C_e}{Q_m k_{ads}} = \frac{1}{Q_m k_{ads}} + \frac{C_e}{Q_m} \quad (5)$$

From equation 5, the slope of the plot of Ce/q_e versus C_e is linear (for Langmuir adsorption) with slope and intercept equal to $1/Q_m$ and $1/k_{ads}Q_m$ respectively.

The fitness of the Langmuir model for the adsorption of DY dye on wood saw dust is confirmed by the linearity of the plot shown in Fig. 6, whose degree of linearity is 0.9794. Calculated theoretical adsorption capacity is 5.5096 g/mg and is less than the average adsorption capacity of 11.1988 g/mg obtained from experiment. The adsorption was favourable because the value of R_L was less than unity (R_L = 0.072).

Adsorption constant is related to the free energy of adsorption, hence, the calculated Langmuir adsorption constant (k_{ads}) is 0.220749 can be applied to Gibb Helmholtz equation (equation 6)

$$\Delta G^0_{ads} = \Delta H^0_{ads} - T\Delta H^0_{ads} \quad (6)$$

The free energy change obtained from the Langmuir adsorption constant was -12.5625 J/mol, which indicate that the adsorption of the dye is spontaneous and is in the range of values expected for the mechanism of physical adsorption (Pathania *et al*., 2017)

The Freundlich isotherm is based in the assumption that the adsorption takes place on heterogenous surface and the adsorption equation can be written as (Saruchi, & Kumar, 2019)

$$q_e = K_F C_e^{\frac{1}{n}} \quad (7)$$

K_F and n are Freundlich adsorption constants. K_F represents the adsorption capacity while n represents the intensity of the adsorption and shows if the adsorption is linear (n = 1), chemisorption (n<1) or physisorption (n>1) (Dhaif-Allah *et al*., 2020).

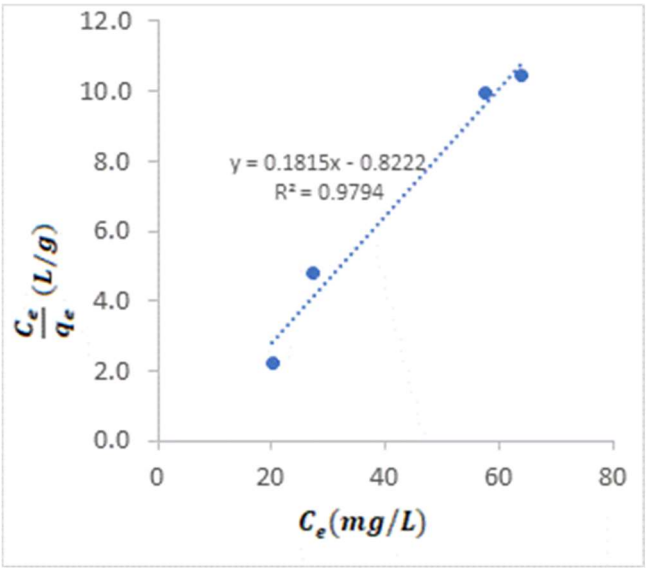

Fig. 6. Langmuir isotherm for the adsorption of DY dye on wood saw dust

The linear model for equation 7 can be developed by taking logarithm of both sides of the equation to obtain equation 8,

$$\boldsymbol{lnq_e} = lnK_F + \frac{1}{n}\boldsymbol{lnC_e} \quad (8)$$

A plot of lnq_e versus lnC_e is expected to give 1/n as the slope and lnK_F if the adsorption obeys the Freundlich model. The obedient of the adsorption of DY dye on wood saw dust to the Freundlich model is signified by the linear plot shown in Fig. 7.

Calculated value of n = 2.05846 which is greater than unity, indicating that the mechanism of adsorption is physical adsorption while the free energy change (calculated from the Freundlich constant) is -14.2237 J/mol, which also confirm physisorption mechanism.

Jovanovic isotherm was also tested for fitness since the Langmuir and Freundlich isotherms did not provide information on the homogeneity and heterogeneity of the adsorption process.

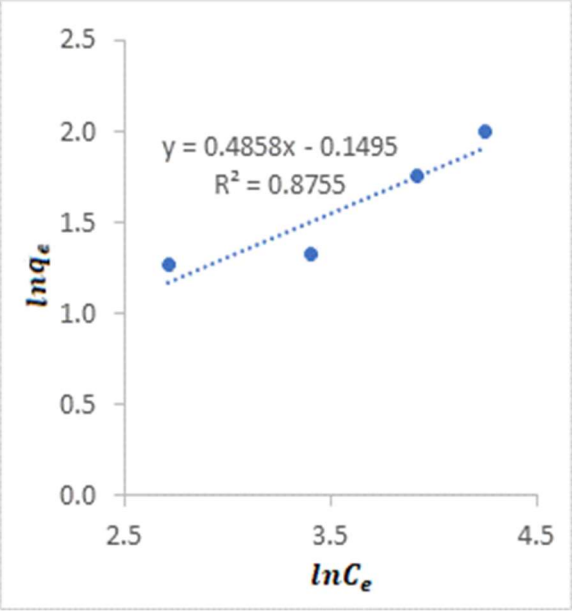

Fig. 7: Freundlich isotherm for the adsorption of DY dye on wood saw dust

The Jovanovic isotherm can be expressed as follows (Shahbeig *et al.*, 2913)

$$q_e = Q_m\left(1 - e^{K_j C_e}\right) \quad (9)$$

The linear form of equation 9 is presented as equation 10

$$lnq_e = lnQ_m - lnQ_m K_j C_e \quad (10)$$

Linear plot of lnq_e against C_e (shown in Fig. 8) confirm the application of Jovanovic model to the adsorption of DY dye on wood saw dust.

Estimated value of lnQ_m is 0. 9946 which gives Q_m = 2.7036, a much lower value than the one obtained from experiment and from the Langmuir plot. The term, k_j is a measure of the deviation from the Langmuir and Freundlich isotherms. Calculated value of k_j was 0.014378. Therefore, there is a monolayer formation without interaction during the adsorption of DY dye on wood saw dust

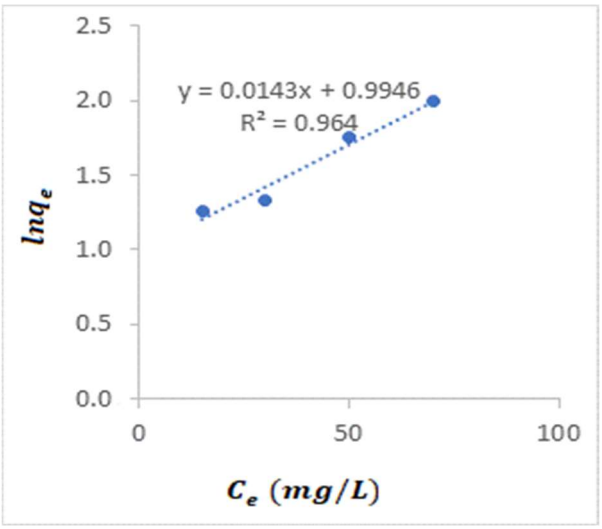

Fig. 8: Javanovic isotherm for the adsorption of DY dye on wood saw dust

Redlich-Peterson isotherm modifies the Langmuir - Freundlich isotherm model by including more constants and a correlation (g) factor signifying, g=0 when it tends to Freundlich and g=1 when it is the Langmuir model (Saruchi & Kumar, 2019). The equation is given below (equation 11) and is simplified to equations 12 and 13.

$$q_e = \frac{A_{RP} C_e}{1 + B_{RP} C_e^g} \quad (11)$$

$$\frac{C_e}{q_e} = \frac{1 + B_{RP} C_e^g}{A_{RP}} = \frac{1}{A_{RP}} + \left(\frac{B_{RP}}{A_{RP}}\right) C_e^g \quad (12)$$

$$ln\left(\frac{C_e}{q_e}\right) = \ln\left(\frac{1}{A_{RP}}\right) + ln\left(\frac{B_{RP}}{A_{RP}}\right) + g lnC_e \quad (13)$$

where A_{RP} and B_{RP} are Redlich-Peterson constants. Calculated value of g for the adsorption of DY dye on wood saw dust was 0.4881 which indicate that the adsorption is tending more to Freundlich isotherm.

Brouers-Sotolongo isotherm (Brouers *et al*. 2005) has two major constants namely, K_{BS} and α. K_{BS} is an index for active site distribution while α represent adsorption power. The general form of the Brouers–Sotolongo model can be written as follows (equation 14)

$$q_e = Q_m[(1 - exp(-k_{BS}(C_e^{\alpha}))] \quad (14)$$

Q_m is the maximum adsorption capacity, k_{BS} and α are Brouers–Sotolongo constants. Estimated value of Q_m from the Brouers–Sotolongo isotherm is 1.2494 while the adsorption power is 0.5119. The adsorption capacity is relatively comparable to those obtained from other isotherms.

3.5 Adsorption kinetic

The expression for the pseudo first and second order kinetic models are presented in equations 15 and 16 respectively (Odoemelam *et al*., 2018)

$$ln(q_e - q_t) = lnq_e - k_1 t \quad (15)$$

$$\frac{t}{q_t} = \frac{1}{k_2 q_e^2} + \frac{t}{q_e} \quad (16)$$

Equation 15 reveals that a plot of $ln(q_e - q_t)$ versus t should be linear if a pseudo first order kinetic is obeyed. Pseudo first order kinetic plot for DY dye is presented in Fig. 9 while adsorption parameters deduced from the plots are recorded in Table 1. Also, from equation, 16 a plot of $\frac{t}{q_t}$ versus t should be linear with slope and intercept approximately equal to $1/q_e$ and $\frac{1}{k_2 q_e^2}$. Pseudo second order plot for DY dyes is also shown in Fig.9 and the adsorption parameters deduced from the plots are also presented in Table 1

.

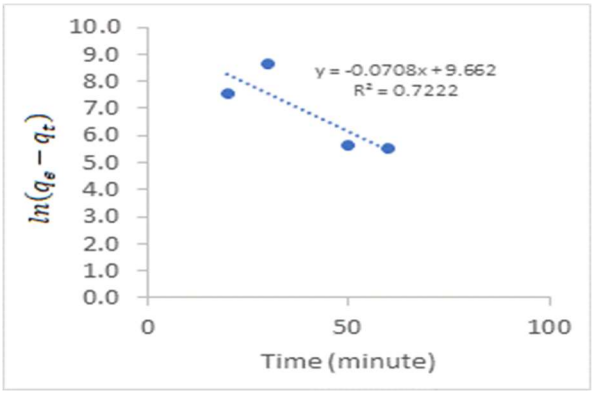

Fig. 9: Pseudo first order kinetic plot for the adsorption of EY and DY dye

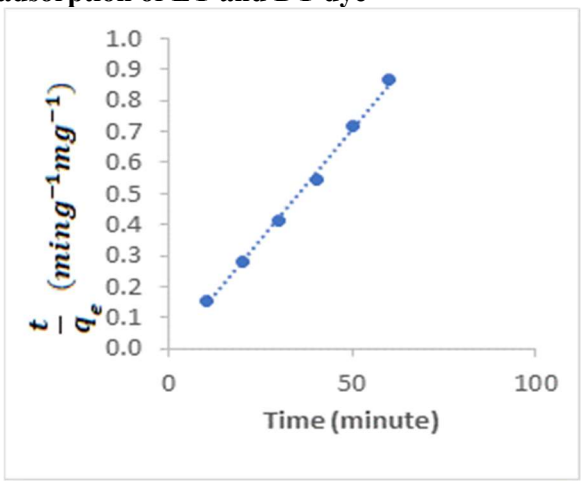

Fig. 10: Pseudo second order kinetic plot for the adsorption of DY dye onto wood saw dust

The results indicated that theoretical adsorption capacities deduced from pseudo first and second order plots for DY dye is comparable to range of values reported for some good adsorption process. Interestingly, the initial adsorption rate (i.e. h) and half adsorption time ($t_{0.5}$) can be derived from the pseudo second order kinetic parameters. Consequently, $h = \frac{1}{k_2 q_e^2}$ and $t_{0.5} = \frac{1}{k_2 q_e}$ respectively and the results are also presented in Table 1. These values are also comparable to those obtained for some good adsorbents

The commonest controlling mechanism for adsorption is diffusion control which can be modelled using Weber and Morris intraparticle diffusion model expressed in equation 17 (Albadarin *et al.,* 2017)

$$q_t = t^{0.5} k_1 \quad (17)$$

k_1 is the intraparticle diffusion constant expressed in mg/g/second$^{0.5}$ and the intercept represent the boundary layer effect. Fig. 11 shows the intraparticle diffusion plot for the adsorption of DY dye on wood saw dust.

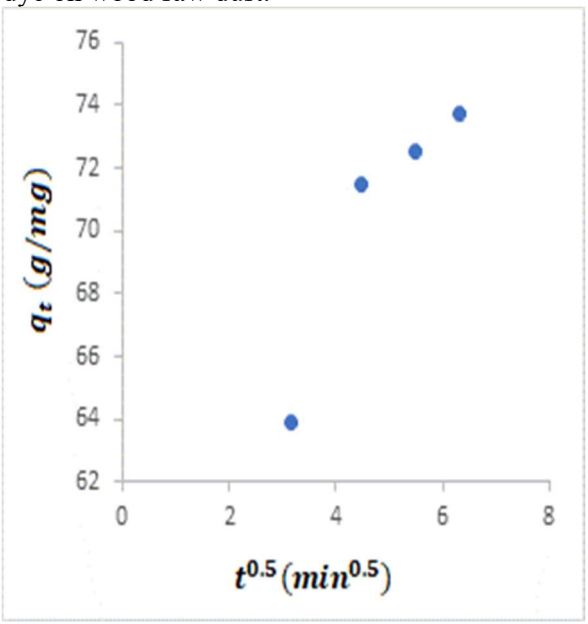

Fig. 11: Intra particle diffusion plots for the adsorption of DY dye

The intercept of the plot is not equal to zero, therefore, the adsorption of the dye is diffusion control. The intra particle rate constant for the first stage is 0.114 mg/g/second$^{0.5}$ while the boundary layer factor is 14.002. However, in the second stage, the rate constant decreases to 0.0316 mg/g/second$^{0.5}$ while the boundary layer parameter increases to

17.263. The first stage in the adsorption is diffusion of the dye to the surface of the adsorbent while the second stage represent the adsorption of the dye on the adsorbent surface. Since the intraparticle rate constant for diffusion is higher, the process is diffusion control and the rate of adsorption is control by the rate at which the adsorbate diffuses to the surface of the adsorbent (Kumar *et al*., 2013).

3.6 FTIR study

The FTIR of DY dye is shown in Fig. 12 while that of the wood saw dust before and after adsorption of DY dye are shown in Fig. 13 and 14 respectively. Observed frequencies of infra-red absorption were 3331 cm^{-1-} with intensity of 42.04, 2140 cm^{-1} with intensity of 95.73 and 1640 cm^{-1} with intensity of 64.80 respectively. These are assigned to hydroxyl group/C-H stretch, S-O stretches respectively.

Table 1: Pseudo first and second order kinetic parameters

Dye	Pseudo first order			Pseudo second order			h	$t_{0.5}$
	k_1	lnq_e	R^2	q_e	k_2	R^2		
DY	0.001	2.996	0.9965	70.42	0.07755	0.9965	0.026	0.1831

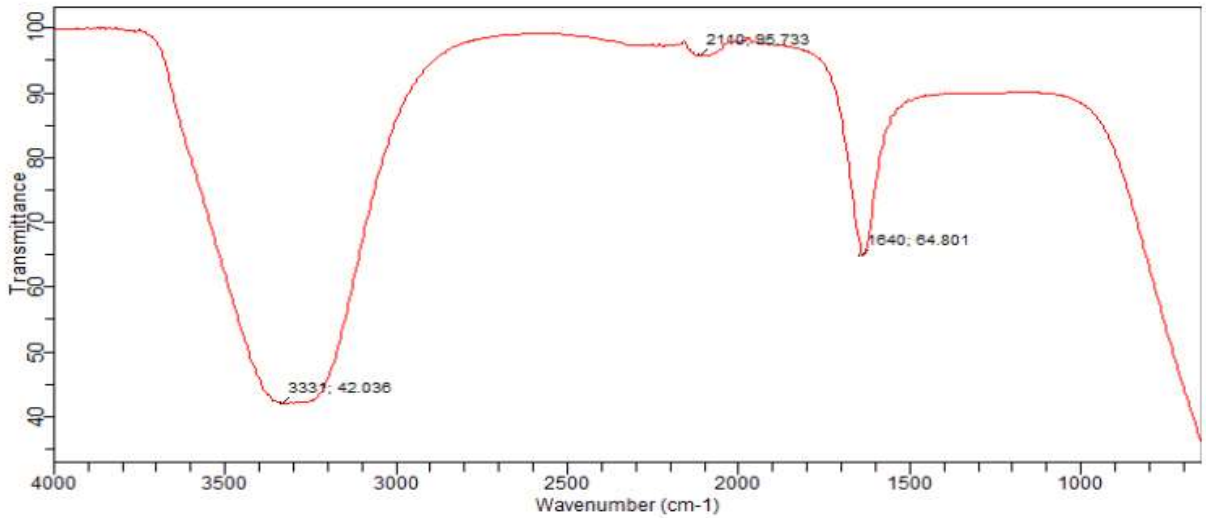

Fig. 12: FTIR of DY dye

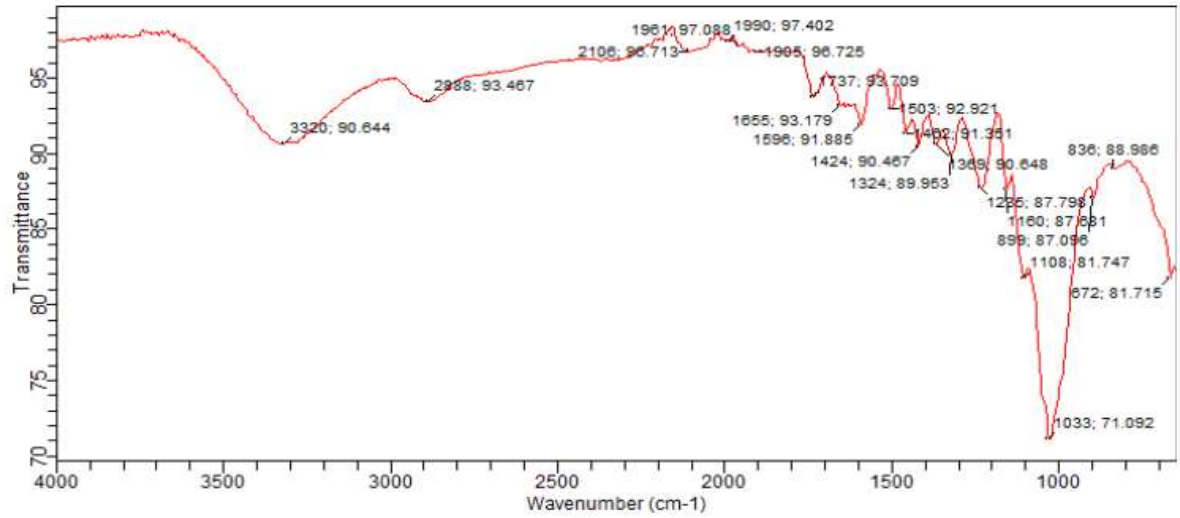

Fig. 13: FTIR of wood saw dust

The spectrum of the wood saw dust displayed functional groups shown in Table 2. However, after adsorption of DY dye, C=C=C stretch at 1990 cm^{-1}, C=O stretch at 1655 cm^{-1}, the C-O stretch at 1286 cm^{-1} were missing in the spectrum of adsorbent indicating that they might have been used for adsorption (Eddy *et al., 2011*). However new functional groups were also found in the spectrum of the adsorbent including OH stretch at 3697 cm^{-1}, C=C stretch at 2184 $cm^{-1,}$ C=C=N stretch at 2009 cm^{-1}, C-O stretches due to adsorption at 2166, 2132, 2002 and 1238 cm^{-1} respectively. These functional groups were used in adsorption (Essien *et al*. (2020)). Other functional groups that retain their infra-red adsorption frequencies experienced enhancement in intensity of adsorption (except for C-O absorption at 1737 cm^{-1} which experienced decrease in intensity) as indicated in Table 2. Shift in frequency is a consequence of existing of interaction (Eddy *et al*., 2008, 2009)

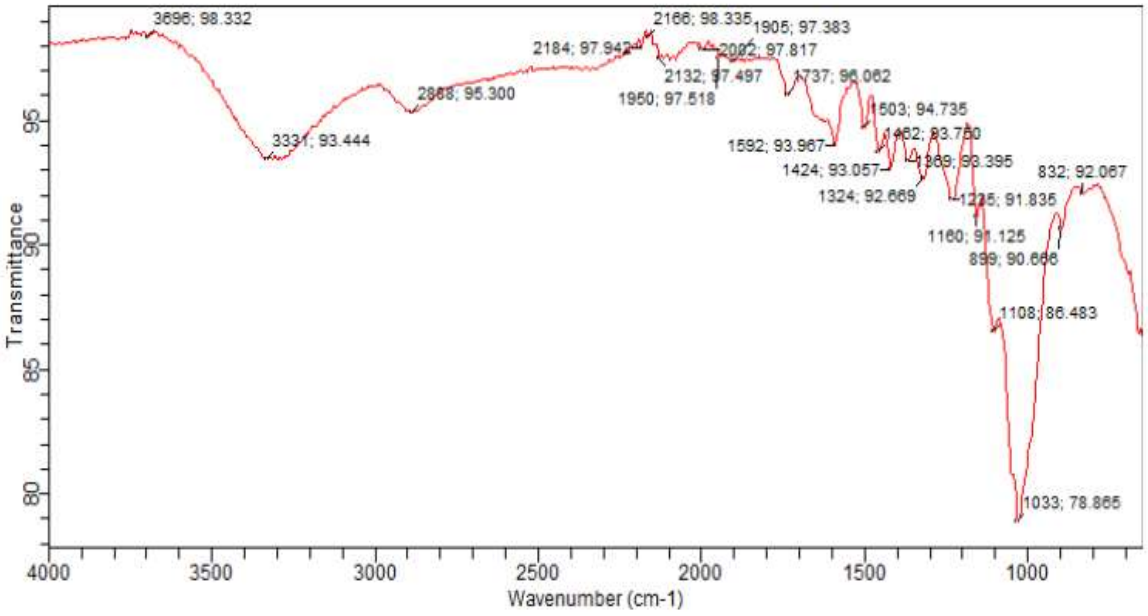

Fig. 14: FTIR spectrum of wood saw dust after adsorption of DY dye

Table 2: Wave number and intensity of IR absorption by wood saw dust before and after adsorption of EY dye

Wood saw dust		**Wood saw dust after adsorption**		**Assignment**
Wave number (cm^{-1})	**Intensity**	**Wave number (cm^{-1})**	**Intensity**	
		3697	98.33	OH stretch
3320	80.64	3331	93.44	OH stretch
2988	93.47	2868	95.3	C-H stretch
		2184	97.94	C≡C stretch
		2166	98.346	C-O stretch
		2132	98.50	C-O stretch
2106	96.13	2117	97.10	Symmetry C=O stretching
		2009	97.61	C=C=N stretch
		2002	97.82	C-O stretch
1990	97.40			C=C=C stretch
1961	96.71	1950	97.52	C=C=C stretch

1905	96.73	1905	97.38	C=C=C stretch
1737	93.71	1737	90.00	C=O stretch
1655	93.18			C=O stretch
1596	91.89	1592	93. 97	C=N stretch
1503	92.92	1503	94.74	C=O stretch
1482	91.35	1462	93.72	C=C stretch
1424	90.47	1424	93.06	OH bending
1369	90.65	1369	93.40	S=O stretch
1324	89.95	1324	92.67	S=O stretch
1286	87.80			C-O stretch
		1235	91.84	C-O stretch
1160	87.68	1160	91.13	C-O stretch
1108	81.75	1108	86.48	C-O stretch
1033	71.09	1033	78.87	C-OH stretch
		899	90.67	C-H bend
836	88.99	832	92.07	C-Cl stretch
672	81.72			C-Br stretch

4.0 Conclusion

The results and findings of the study indicated that the wood saw dust is an efficient adsorbent for DY dye. The adsorption of the dye is spontaneous and obey several adsorption isotherms. FTIR study indicated that the major functional groups in the wood sawdust that aided the adsorption were C-O and C=O stretches. Commercial utilization of this dye for decolourizing DY dye contaminated water can be tested and implemented.

5.0 References

Albadarin, A. B., Collins, M. N., Naushad, M., Shirazian, S., Walker, G. & Mangwandi, C. (207). Activated lignin-chitosan extruded blends for efficient adsorption of methylene blude dye. *Chemical Engineering Journal,* 307, 1, pp. 264-272.

Banerjee, S. & Chattopadhyaya, M. C. (2017). Adsorption characteristics for the removal of a toxic dye, tartrazine from aqueous solutions by a low cost agricultural by product, *Arabian Journal of Chemistry,* 10, pp. S1629-S1638.

Chiu, C., Wu, M., Lee. C. & Cheng, T. (2018). Isothermal adsorption properties for the adsorption and removal of reactive blue 221 dye from aqueous solutions by cross-linked β-chitosan glycan as acid resistant adsorbent. *Polymers*, 10, 1328; doi:10.3390/polym10121328

Dhaif-Allah, M. A. H., Taqui, S. N., Syed, U. T, & Syed, A. A. (2020). Kinetic and isotherm modelling for acid blue 113 dye adsorption onto; low cost nutraceutical fenugreek seed spent. *Applied Water Science,* 10, 58, https://doi.org/10.1007/s13201-020-1141-3.

Eddy, N. O. (2009). Modelling of the adsorption of Zn^{2+} from aqueous solution by modified and unmodified *Cyperus esculentus* shell. *Electronic Journal of Environmental, Agriculture. & Food Chemistry* 811: 1177-1185.

Eddy, N. O., Ameh, P., Gimba, C. E. & Ebenso, E. E. (2011). GCMS studies on *Anogessus leocarpus* (AL) gum and their corrosion inhibition potentials for mild steel in 0.1 M HCl. *International Journal of Electrochemical Sciences* 6, pp.5815-5829.

Eddy, N. O., Ameh, P., Gimba, C. E. & Ebenso, E. E. (2011a). GCMS studies on *Anogessus leocarpus* (AL) gum and their corrosion inhibition potentials for mild steel in 0.1 M HCl. *International Journal of Electrochemical Sciences,* 6, pp. 5815-5829.

Eddy, N. O., Ekwumengbo, P. A. & Mamza, P. A. P. (2009). Ethanol extract of *Terminalia catappa* as a green inhibitor for the corrosion of mild steel in H_2SO_4. *Green Chemistry Letters and Review* 2, 4, pp. 223-231.

Eddy, N. O., Ita, B. I., Dodo, S. N. & Paul, E. D. (2011). Inhibitive and adsorption properties of ethanol extract of *Hibiscus sabdariffa* calyx for the corrosion of mild steel in 0.1 M HCl. *Green Chemistry Letters and Review,* 5, 1, pp. 43-53.

Eddy, N. O., Ita, B. I., Dodo, S. N. & Paul, E. D. (2011b). Inhibitive and adsorption properties of

ethanol extract of *Hibiscus sabdariffa* calyx for the corrosion of mild steel in 0.1 M HCl. *Green Chemistry Letters and Review,* 5, 1, pp.43-53.

Eddy, N. O., Odoemelam, S. A. & Odiongenyi, A. O. (2008). Ethanol extract of *Musa acuminate* peel as an eco-friendly inhibitor for the corrosion of mild steel in H_2SO_4. *Advances in Natural and Applied Sciences,* 2, 1, pp. 35-42.

Ekop, A. S. & Eddy, N. O. (2010). Chermodynamic study on the adsorption of Pb^{2+} and Cd^{2+} from aqueous solution by human hair. *E. Journal of Chemistry* 7(4): 1296-1303.

El Boujaady, H., Mourabet, M., Bennani-Ziatni, M. & Taitai, A. (2014). Adsorption/desorption of direct yello 28 on apatitic phosphate: mechanism, kinetic and thermodynamic studies. *Journal of the Association of Arab Universities for Basic and Applied Sciences*, 16, pp. 64-73.

Essien, N. B., Essien, U. & Ibuot, A. A. (2020). Sorghum waste as an efficient adsorbent for the removal of $zn^{2+}$and cu^{2+} from aqueous medium. *Communication in Physical Sciences, 5, 2, pp. 51-61.*

Gupta, N., Kushwaha, A. K. & Chattopadhyaya, M. C. (2016). Application of potato (*Solanum tuberosum)* plant wastes for the removal of methylene blue and malachite green dye from aqueous solution. *Arabian Journal of Chemistry*, 9, S707-S716.

Gupta, N., Kushwaha, A. K. & Chattopadhyaya, M. C. (2016). Application of potato (*Solanum tuberosum*) plant wastes for the removal of methylene blue and malachite green dye from aqueous solution. *Arabian Journal of Chemistry,* 9, 1, pp. S707-S716.

Iqbal, J., Wattoo, F. H., Wattoo, M. H. S., Malik, R., Tirmizi, S. A., Imran, M & Ghangro, A. B. (2011). Adsorption of acid yellow dye on flakes of chitosan prepared from fishery wastes *Arabian Journal of Chemistry*, 4, 4, pp. 389-395

Kuang, Y., Zhang, X. & Zhou, S. (2020). Adsorption of methylene blue in water onto activated carbon by surfactant modification. *Water* 2020, 12, 587; doi:10.3390/w12020587

Kumar, P. S., Fernando, P. S.A., Ahmed, R. T., Srinath, R., Priyadharshini, M., Vignesh, A. M. And Thanjiappan, A. (2013). Effect of temperature on the adsorption of methylene blue dye onto sulfuric acid-treated orange peel. *Chemical Engineering Communication* 201:1526-1547.

Lafi, R., Montasser, I. & Hafian, A. (2019). Adsorption of congo red dye from aqueous solutions by prepared activated carbon with oxygen containing functional groups and its regulation. *Adsorption Science and Technology*, 37, 1-2, pp. 160-181.

Miyah, Youssef, Y., Lahrichi, A., Idrissi, M.,Boujraf, S., Taouda, H. & Zerrouq, F. (2017). Assessment of adsorption kinetics for the removal potential of crystal violet dye from aqueous solution using Moroccan pyrophyllite. *Journal of the Association of Arab Universities for Basic and Applied Sciences*, 23, pp.20-28

Munagapati, V. S., Kim, V. Y. Y., Lee, K. M. & Kim, D. (2018). Removal of anionic dyes (Reactive Black 5 and Congo Red) from aqueous solutions using Banana Peel Powder as an adsorbent.

*Odiongenyi, A. O. & Afangide, U. N. (2019). A*dsorption and thermodynamic studies on the removal of congo red dye from aqueous solution by alumina and nano-alumina. *Communication in Physical Sciences*, 4, 1, pp. 1-7.

Odiongenyi, A. O. (2019). Rremoval of ethyl violet dye from aqueous solution by graphite dust and nano graphene oxide synthesized from graphite dust. *Communication in Physical Sciences*, 4, 2, pp. 103-109.

Odoemelam, S. A. & Eddy, N. O. (2009). Studies on the use of oyster, snail and periwinkle shells as adsorbents for the removal of Pb^{2+} from aqueous solution. *E. Journal of Chemistry* 6, 1, pp. 213-222

Odoemelam, S. A., Emeh, U. N. and Eddy, N. O. (2018). Experimental and computational chemistry studies on the removal ofmethylene blue and malachite green dyes from aqueous solution by neem (*Azadirachta Indica*) leaves. *Journal of Taibah University for Science* 12, pp. 255-265.

Palapa, N. R., Mohadi, R. & Lesbani, A. (2018). Adsorption of direct yellow dye from aqueous solution by Ni/Al and Zn/Al layered double hydroxides. AIP Conference Proceedings, https://doi.org/10.1063/1.5064978

Pathania, D., Sharma, S. & Singh, P. (2017). Removal of methylene blue by adsorption onto activated carbon developed from *Ficus carica*

blast. *Arabian Journal of Chemistry,* 10, 1, pp. S1445-S1451.

Revathi, G., Ramalingam, S. & Surramaniam, P. (2011). Kinetics of adsorption of direct yellow 12 dye from aqueous solution by jack fruit leaf carbon. *International Journal of Chemical Sciences*, 9, 2, pp.524-,536.

Saruchi, & Kumar, V. (2019). Adsorption kinetics and isotherms for the removal of rhodamine B dye and Pb^{2+} ions from aqueous solutions by hybrid ion-exchanger. Arabian Journal of Chemistry, 12, 1, pp. 316-329

Shahbeig, H., Baghen, N., Ghorbanian, S. A., Hallajisani, A. & Poorkarium, S. (2013). A new adsorption isotherm modek of aqueous solutions on granular activated carbon. World Journal of Modelling and Simulation , 9, 4, pp. 243-254

Shoukat, S., Bhatti, H. N., Iqbal, M. & Noren, S. (2017). Mango stone bio composite preparation and application for crystal violet adsorption: A mechanistic study. *Microporous and Mesoporous Materials*, 239, 180-189.

Silva, C. E. D., da Gama, B. M. V., Goncalves, A. H. D., Medeiros, J. A. & Abud, A. K. D. (2019). Basic dye adsorption in albedo residue: effect of contact time, temperature, dye concentration, biomass dosage, rotation and ionic strength. *Journal of King Saud University-Engineering Sciences,* https://doi.org/10.1016/j.jksues.2019.04.006

Weloye, J. N., Wanyonyi, W. C., Wangila, P. T. & Tonui, M. K. (2020). Kinetic and equilibrium studies of Congo red dye adsorption on cabbage. *Environmental Chemistry and Ecotoxicology,* 2, pp. 24-31.